Performances of a protector against scattered radiation during intraoperative use of a C-arm fluoroscope

2016 J. Radiol. Prot. 36 629

(http://iopscience.iop.org/0952-4746/36/3/629)

IOP Publishing | Society for Radiological Protection Journal of Radiological Protection

J. Radiol. Prot. **36** (2016) 629–640 doi:10.1088/0952-4746/36/3/629

Performances of a protector against scattered radiation during intraoperative use of a C-arm fluoroscope

Ki Hyuk Sung[1,6], Young-Jun Jung[2,6], Soon-Sun Kwon[3], Gye Wang Lee[4], Chin Youb Chung[1], Kyoung Min Lee[1], Hyemi Cha[2], Moon Seok Park[1,7,9] and Kisung Lee[2,5,7,8]

[1] Department of Orthopaedic Surgery, Seoul National University Bundang Hospital, 300 Gumi-Dong, Bundang-Gu, Seongnam, Gyeonggi 13620, Korea
[2] Department of Bio-convergence Engineering, Korea University, 145 Anam-ro, Seongbuk-gu, Seoul 02841, Korea
[3] Department of Mathematics, College of Natural Sciences, Ajou University, 206 Worldcup-ro, Yeongtong-gu, Suwon, Gyeonggi 16499, Korea
[4] Department of Orthopaedic Surgery, DK Dongcheon Hospital, 215 Oesolkeun-gil, Jung-gu, Ulsan 44495, Korea
[5] School of Biomedical Engineering, Korea University, 145 Anam-ro, Seongbuk-gu, Seoul 02841, Korea

E-mail: kisung@korea.ac.kr and pmsmed@gmail.com

Received 10 March 2016, revised 20 July 2016
Accepted for publication 22 July 2016
Published 12 August 2016

Abstract

The scattered radiation protector for mobile x-ray systems, Creative Valuable Protector-2, has been recently developed. However, there have been no studies investigating the effects of this device. We aim to investigate the effects of the scattered radiation protector on the equivalent doses from scattered radiation delivered to radiosensitive organs while simulating spine surgery using a C-arm fluoroscope. Chest and rando phantoms were used to simulate a patient and a surgeon in this study. The equivalent dose from scattered radiation to radiosensitive organs was measured in four different situations according to the use of the scattered radiation protector and the C-arm configuration. To compare the quality of the images with and without the scattered radiation protector, an acryl step phantom with five steps was used, and the contrast resolution of each step was calculated. The equivalent dose from the scattered radiation to the surgeon's eye, thyroid, and gonad decreased significantly

[6] Contributed equally to the writing of this article.
[7] Authors to whom any correspondence should be addressed.
[8] School of Biomedical Engineering, Korea University, 145 Anam-ro, Seongbuk-gu, Seoul 02841, Korea.
[9] Department of Orthopaedic Surgery, Seoul National University Bundang Hospital, 300 Gumi-Dong, Bundang-Gu, Sungnam, Kyungki 13620, Korea.

0952-4746/16/030629+12$33.00

by using the scattered radiation protector for both the Posteroanterior (PA) ($p < 0.001$) and Anteroposterior (AP) ($p < 0.001$) C-arm configurations. The installation of the scattered radiation protector also reduced the direct radiation dose to the chest phantom. A scattered map showed that scattered radiation doses decreased by approximately 50% for the PA configuration and 75% for the AP configuration by using the scattered radiation protector. Before and after installation of the scattered radiation protector, the contrast resolution of each adjacent step area was 0.025–0.404 and 0.216–0.421. The scattered radiation protector was effective in reducing not only the equivalent dose from scattered radiation to the surgeon's radiosensitive organs, but also the direct radiation dose to the patient. This was all achieved without decreasing the quality of the C-arm fluoroscopic images.

Keywords: C-arm fluoroscope, scattered radiation protector, equivalent dose from scattered radiation, photoluminescence dosimeter

(Some figures may appear in colour only in the online journal)

Introduction

X-ray fluoroscopy imaging systems have been widely used for many orthopedic procedures in operating rooms and emergency rooms. Of these, the C-arm fluoroscope is widely used intraoperatively by orthopedic surgeons because it displays real-time moving images of skeletal structures (Giordano *et al* 2007, Lee *et al* 2012, Park *et al* 2012). The real-time imaging capabilities of C-arm fluoroscopy provide considerable temporal anatomical information (Dawe *et al* 2011, Lee *et al* 2011). For instance, surgeons can confirm the reduction of fractures and the accurate placement of radio-opaque implants (Giordano *et al* 2007). In addition, fluoroscopy is widely used to guide various interventional procedures, such as angiography, pyelography, barium enema, and facet injection. This results in early functional recovery, reduced hospital stay, and consequent cost (Rubesin *et al* 2000, Gavit *et al* 2007, Das *et al* 2015, Huang 2016).

However, operators are actually exposed to scattered radiation as long as the beam is on, and can be exposed to direct radiation from the C-arm fluoroscope if their hands cross the beam (Miller *et al* 2010, Rehani *et al* 2010). Therefore, there are growing concerns regarding the amount of radiation received during the use of a C-arm fluoroscope (Mesbahi and Rouhani 2008, Shoaib *et al* 2008, Tuohy *et al* 2011). Organs sensitive to radiation include the gonads, bone marrow, breasts, cornea, gastrointestinal tract, lungs, and thyroid. In particular, the breasts and thyroid of a surgeon are exposed to the most scattered radiation when performing intraoperative C-arm fluoroscopy (Biswas *et al* 2009, Lee *et al* 2012).

Several studies have investigated the radiation doses received from C-arm fluoroscopy (Athwal *et al* 2005, Giordano *et al* 2007, 2009, Shoaib *et al* 2008, Rehani *et al* 2010, Lee *et al* 2012, Sung *et al* 2016). They showed that the following factors could reduce radiation exposure during the intraoperative use of C-arm fluoroscopy: (1) the use of a mini C-arm instead of the conventional C-arm; (2) the avoidance of direct radiation exposure; (3) the configuration of the C-arm; (4) the distance between the C-arm and the surgeons; (5) the use of radioprotective equipment; (6) reducing the exposure time; (7) placing a shielded screen between the radiation source and the surgeons; and (8) rotating the surgeons' eyes away from the patient. Most surgeons use protective garments, such as lead aprons and thyroid shields, in order to decrease the scattered radiation exposure during spine surgery. However, concerns have been raised regarding the toxicity of lead, and discomfort owing to their heavy weight.

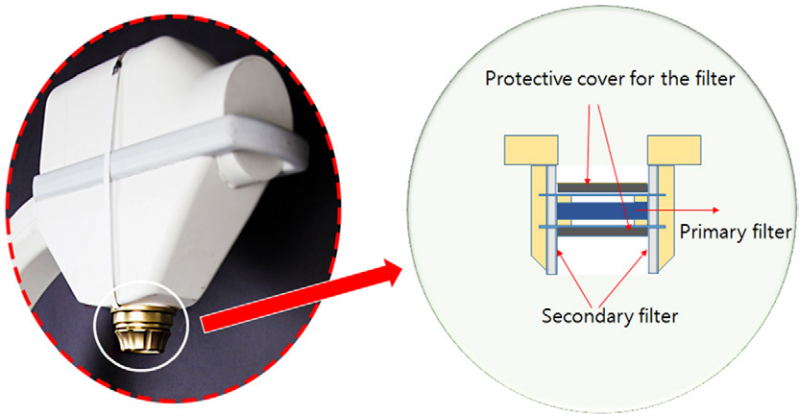

Figure 1. Diagram of the scattered radiation protector (white circle), which is composed of primary and secondary filters made from a specific type of ceramic.

A scattered radiation protector for mobile x-ray systems, known as Creative Valuable Protector-2 (CVP-2), has recently been developed and underwent standard lab testing in 2012. This device was registered and listed by the Food and Drug Administration in 2014 but has not yet been widely used (US Food and Drug Administration 2016, Input the 'msline' in the Establishment Name). CVP-2 is composed of two layers of filters made from specific types of ceramic. The scattered radiation protector allows transmission of the short-wavelength band of x-rays generated from the x-ray tube to form images. Meanwhile, the primary filter significantly decreases the x-ray exposure of patients and medical staff by filtering long-wavelength x-rays, which causes scattering, refraction, and reflection to the patients' body. In addition, the secondary filter reduces the radial x-ray exposure from the x-ray tube (figure 1). Therefore, this device is expected to decrease the scattered radiation dose to radiosensitive organs, and furthermore to be more comfortable to surgeons (as compared to using protective garments).

However, there have been no studies investigating the performances of the scattered radiation protector. Therefore, we performed this study in order to investigate the performances of the newly developed scattered radiation protector on the equivalent doses from scattered radiation delivered to radiosensitive organs while simulating spine surgery using a C-arm fluoroscope. In addition, we compared the quality of C-arm fluoroscopic images that were obtained with and without the use of the scattered radiation protector.

Methods

This study was exempted from the approval of the institutional review board at our institute because it involved no human subjects.

Two phantoms, a chest and a rando phantom, were used to simulate a patient and a surgeon in this study. The anthropomorphic chest phantom (RS-111; Radiology Support Devices, Long Beach, CA, USA) that was used to simulate the patient was located on the operating table. The chest phantom was composed of a cadaver bone surrounded by soft-tissue-equivalent acrylic material. Thus, it had approximately the same density as human soft tissue. A C-arm fluoroscopy unit (OEC 9800; GE Healthcare, Milwaukee, WI, USA) was positioned beside the chest phantom at a 90° angle. The distance between the chest phantom on the operating table and the x-ray tube was 40 cm. The fluoroscopic screen was focused on the xyphoid process. The C-arm fluoroscopic operating parameters were 80 kVp and 5.00 mA. The rando phantom (ART200-5;

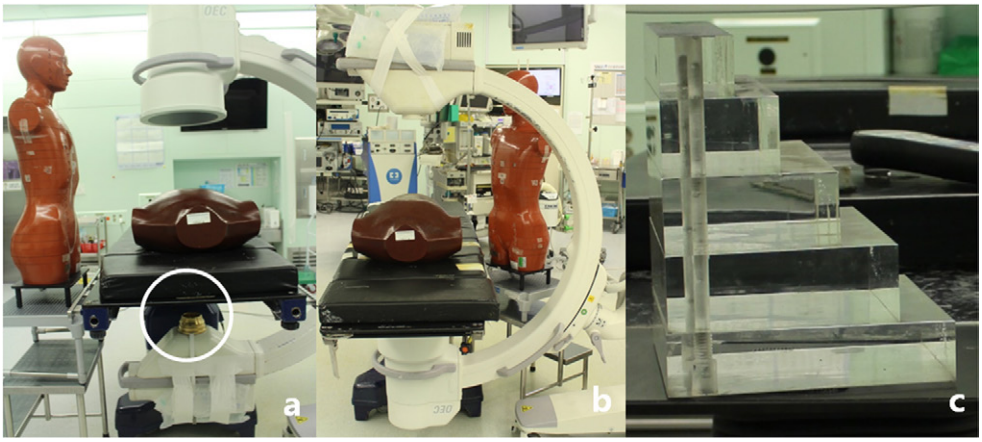

Figure 2. Experimental setup for radiation dose measurements. (a) Rando phantom (the main operator) is located at an angular position of 90°, and the C-arm is in the standard PA configuration with the scattered radiation protector (white circle). (b) Rando phantom (the first assistant) is located at an angular position of 215°, and the C-arm is in the inverted AP configuration without the scattered radiation protector. (c) The acryl step phantom contains five steps; the heights of the first and fifth steps were 4 cm, whereas the others were 5 cm.

Radiology Support Devices, Long Beach, CA, USA) that simulated the surgeon was placed beside the chest phantom at a distance of 50 cm. The rando phantom was located at an angular position of 90° (the opposite side of the C-arm fluoroscope) in order to simulate the main operator, or at an angular position of 215° in order to simulate the first assistant. The height of the operator phantom was adjusted to 173 cm in order to simulate a standing position.

Photoluminescence dosimeters (GD-352M; AGC Techno Glass, Tokyo, Japan) were inserted into the rando phantom at the positions of the eye, thyroid, and gonad so that the radiation exposure could be measured at the most critical regions of the surgeon's body. The photoluminescence dosimeters were placed at 10, 24, and 79 cm from the top of the head to represent the surgeon's eye, thyroid, and gonad. In addition, a photoluminescence dosimeter was attached to the sternum of the chest phantom to measure the direct surface radiation dose delivered to the patient.

CVP-2 (MS Line ENG Co., Ltd, Seoul, Korea), the scattered radiation protector for mobile x-ray systems, was used to investigate the extent of the protection offered against scattered radiation. Equivalent scattered radiation doses were measured for two C-arm configurations, which were the standard Posteroanterior (PA) configuration (with the x-ray tube located downward, and the detector located upward) and the inverted Anteroposterior (AP) configuration (with the x-ray tube located upward, and the detector located downward). Therefore, equivalent scattered radiation doses to sensitive organs were measured in four different scenarios according to the use of the scattered radiation protector and the configuration of the C-arm (figures 2(a) and (b)).

The chest phantom was exposed to the radiation source for 10 min with the chest and operator phantoms placed together, and the surface radiation dose accumulated in the photoluminescence dosimeters on the eye, thyroid, and gonad of the operator phantom. In addition, direct surface radiation doses delivered to the chest phantom were measured using photoluminescence dosimeters. A dosimeter was attached to the sternum of the chest phantom in the AP configuration, and the back of the chest phantom in the PA configuration, to compare the direct surface radiation dose delivered to the patient according to the C-arm configuration. Each experimental scenario was repeated five times.

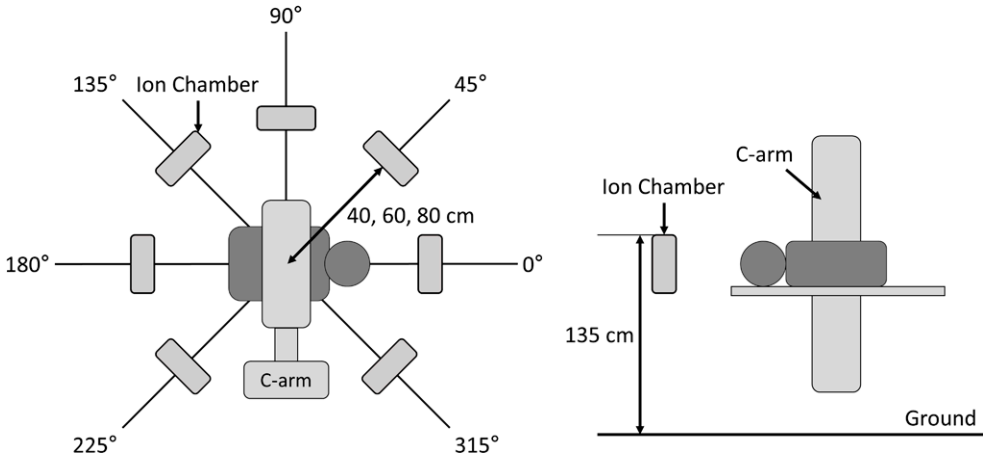

Figure 3. Locations of the ion chamber in relation to the C-arm and the chest phantom for the measurement of the air kerma rate. Top view (left) and lateral view (right).

The air kerma rate was measured as a scattered radiation dose using a digital radiation survey meter (Victoreen 660, Fluke Biomedical, WA, US) during 1 min of continuous use of the C-arm fluoroscope. This measurement was performed at horizontal distances of 40 cm, 60 cm, and 80 cm from the xiphoid process of the chest phantom and at angular positions of 0°, 45°, 90°, 135°, 180°, 225°, and 315°. The air kerma rate as a scattered radiation dose was recorded at each measurement position (figure 3).

The kerma area product (KAP) was measured to assess the output of the fluoroscopic x-ray source in the C-arm fluoroscopic setting. A KAP meter (VacuTec, Dresden, Germany) was attached to the x-ray tube of the C-arm fluoroscope. A 5 min dose of radiation was applied, and the measured values were converted into units of dose per minute.

To compare the quality of images with and without the use of the scattered radiation protector, the acryl step phantom, which consisted of water-equivalent materials, was placed on the patient's bed. The phantom contained five steps: the heights of the first and fifth steps were 4 cm, whereas the others were 5 cm (figure 2(c)). For the PA configuration, the distance from the image intensifier to the top of the phantom was 3 cm, because every step should be included in the field of view. The tube voltage and current were 80 kVp and 5 mA, respectively, and the exposure time was 3 s. The step phantom images from the C-arm fluoroscope before and after installing the scattered radiation protector had the boxes (25 × 25 pixels) on each step located on the same position (figure 4). We defined the sum of the pixel values in the box at its area as S_i. The contrast resolution (CR) described the difference between two target regions of interest (Prince and Links 2006). The CR of each step was calculated according to the equation below:

$$\mathrm{CR} = (S_i - S_{i+1})/(S_i + S_{i+1}),$$

where S_i and S_{i+1} indicate the values of the signal intensity at each step.

Statistical methods

Prior sample size estimation was performed under assumption of the two-way analysis of variance (ANOVA) model. When we assumed an effect size of 0.85, significance level of 0.05 and power of 0.85, 5 trials were required at the level of each factor.

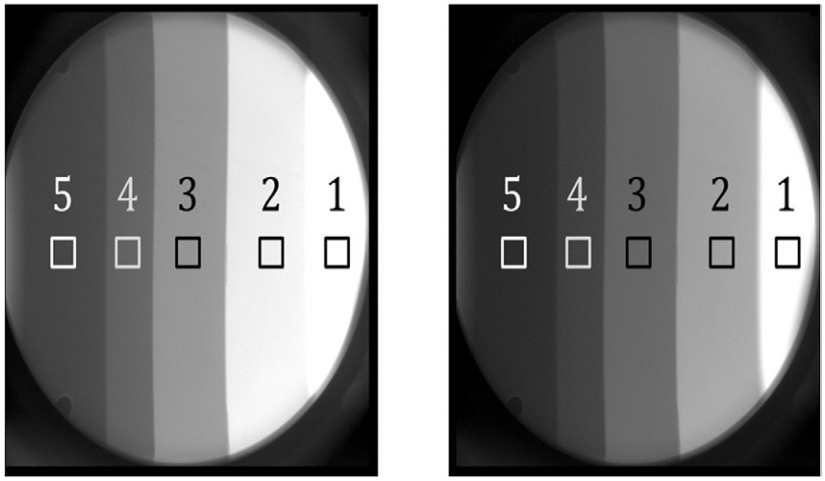

Figure 4. Acryl step phantom images before installation (left) and after installation (right) of the scattered radiation protector. Pixels in the square boxes were used to calculate the contrast resolution (CR).

Factorial ANOVA was used to analyze the differences in equivalent dose from scattered radiation between the two groups based on whether or not the scattered radiation protector was used, and based on the type of sensitive organ in question. Multiple comparison tests were performed using the Bonferroni correction. All statistical analyses were performed using R version 3.2.0 (R Foundation for Statistical Computing, Vienna, Austria). All statistics were two-tailed, and *P*-values of <0.05 were considered to be significant.

Results

The equivalent doses from scattered radiation to the main operator's eye, thyroid, and gonad decreased significantly as a result of using the scattered radiation protector (CVP-2) for both standard PA ($p < 0.001$) and inverted AP C-arm configurations ($p < 0.001$). The equivalent doses from scattered radiation to the first assistant's radiosensitive organs also decreased as a result of using the scattered radiation protector, except for the case of the gonad with the AP configuration. Moreover, the scattered radiation protector reduced the equivalent doses from scattered radiation to the main operator's sensitive organs by 37–57% for the AP configuration, and by 28–37% for the PA configuration. The lowest radiation dose was delivered to the eye for the PA configuration and the gonad for the AP configuration. The equivalent dose from scattered radiation to the radiosensitive organs was lower with the PA configuration than with the AP configuration, except for gonads with the scattered radiation protector (figure 5).

The use of the scattered radiation protector reduced the direct radiation to the patient by 73% for the AP configuration, and by 68% for the PA configuration (table 2).

A scattered map shows that the scattered radiation doses decreased by 50% for the PA configuration and by 75% for the AP configuration as a result of using the scattered radiation protector; furthermore, the scattered radiation doses were greatest at an angle of 180° (figure 6).

The KAP for the C-arm fluoroscope with the scattered radiation protector was significantly lower than that without the scattered radiation protector ($p = 0.008$, table 1).

The CR for each adjacent step area fell in the range of 0.025–0.404 before installing the scattered radiation protector, and shifted to the range of 0.216–0.421 after installing the

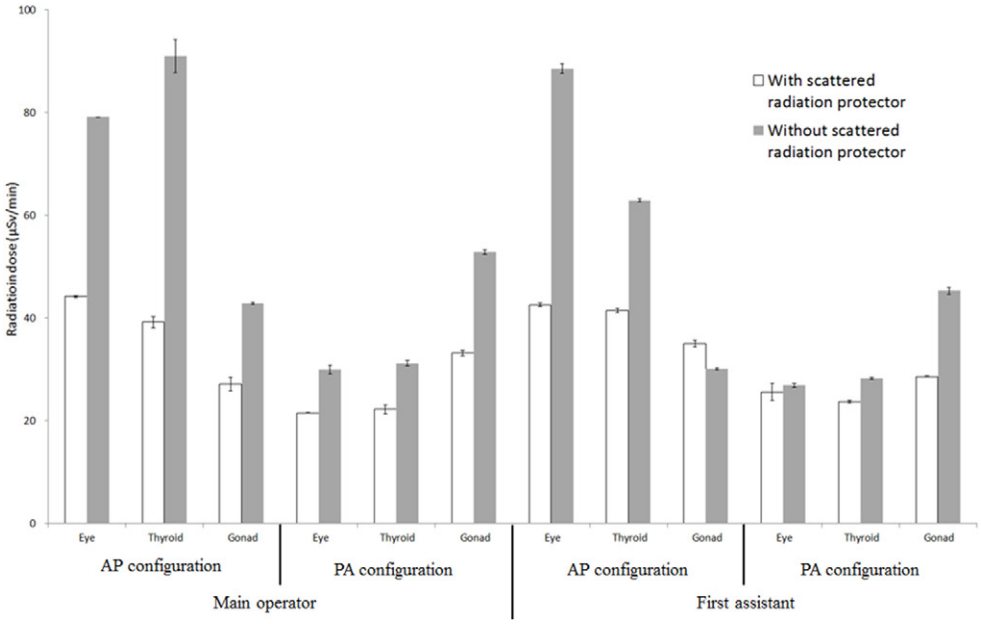

Figure 5. Comparison of equivalent scattered radiation dose exposure to sensitive organs according to the use of the scattered radiation protector and the configuration of the C-arm fluoroscope. The numbers represent mean values of the five measurements conducted.

Table 1. Comparison of direct radiation exposure to the patient with and without the use of the scattered radiation protector.

	AP configuration	PA configuration
With scattered radiation protector	9.8 (SD 0.2)	9.0 (SD 0.5)
Without scattered radiation protector	36.7 (SD 0.9)	28.5 (SD 0.8)

Radiation dose in mSv min^{-1}. The numbers represent mean values of the five measurements conducted.

radiation protector. Even though the C-arm system with CVP-2 irradiated all the organs of the operators and patient with a low exposure dose, the ratio of CRs (with/without the scattered radiation protector) was approximately 1 at steps 2–3, 3–4, and 4–5. In the case of steps 1–2, however, the CR is relatively low (0.025) without CVP-2 because the pixels were saturated in that region. With CVP-2, the primary filter particularly reduced the low-energy x-ray photons, which have long wavelengths, thus improving the CR at steps 1–2 to 0.216 (figure 7).

Discussion

The current study demonstrates that the equivalent dose from scattered radiation to the surgeon's radiosensitive organs, as well as the direct radiation dose to the patient, can be reduced by using the newly developed scattered radiation protector. In addition, our results show that the quality of the C-arm fluoroscopic image does not decrease upon installing the scattered radiation protector.

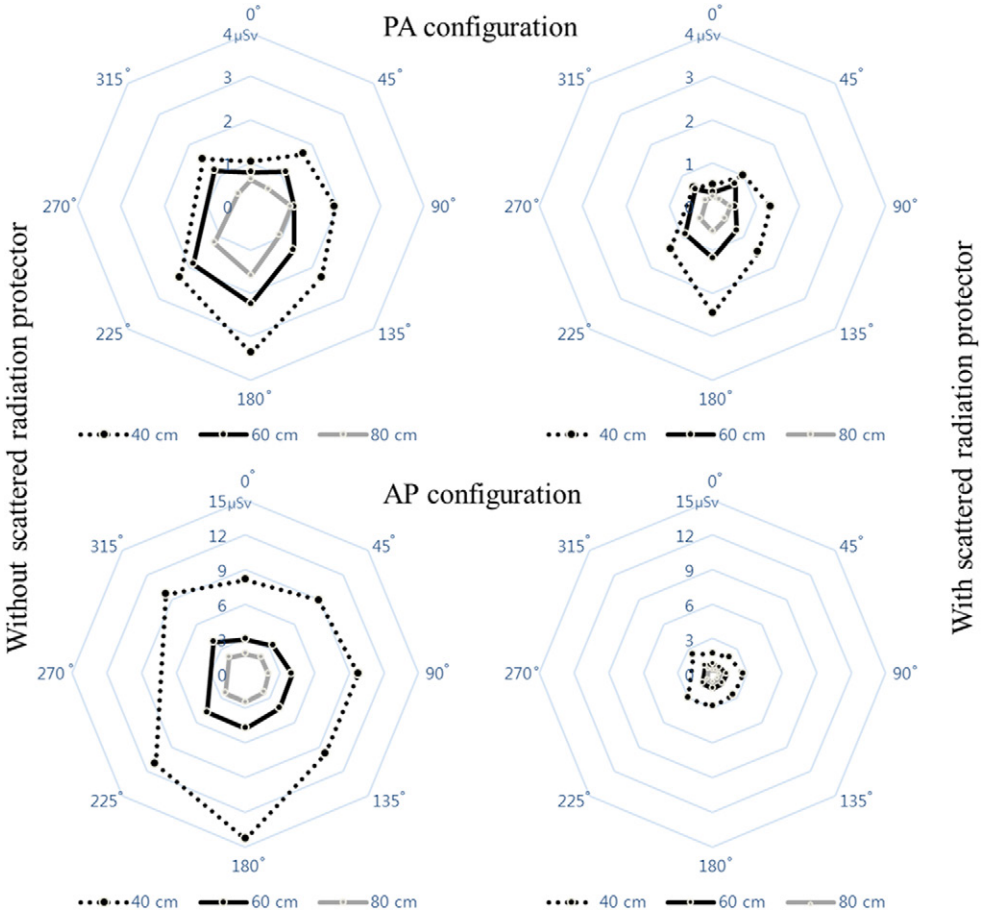

Figure 6. Scatter radiation dose map at positions located at different distances and angles from the center of the chest phantom. Radiation doses were presented in mR (Roentgen). Note that the scatter radiation doses were higher in the AP configuration than in PA because doses were measured in a volume above the table.

Before discussing the implications of the current study, some limitations should be addressed. First, the current study does not compare the effects of the scattered radiation protector against those of protective garments. Therefore, we cannot say that the use of the scattered radiation protector can replace the use of protective garments; further study on this issue is required. Second, the fluoroscopic beam was focused on the xyphoid process in order to simulate spine surgery in this study. Therefore, the results may not be applicable to a variety of other orthopedic procedures.

Lead-shield garments have been widely used in the medical field for radiation protection, including lead aprons, thyroid shields, and protective eyewear. Previous studies have reported that lead-shield garments reduce the scattered radiation dose by 52–96%, depending on the type of C-arm fluoroscope and the radiosensitive organ in question (Shortt *et al* 2007, Lyra *et al* 2011, Lee *et al* 2012, 2013, Goren *et al* 2013, Sung *et al* 2016, Bertolini *et al* 2016). However, these radiation protection garments are very heavy and uncomfortable for surgeons to wear owing to their lead-content, particularly during long-duration surgery. Recent studies have evaluated lead-free radiation shielding materials as a lead substitute because of the

Table 2. Measured KAP of the C-arm fluoroscope.

	KAP (μGym^2 min^{-1})
With scattered radiation protector	101.78 (SD 0.98)
Without scattered radiation protector	371.22 (SD 0.98)

The numbers represent mean values of the five measurements conducted.

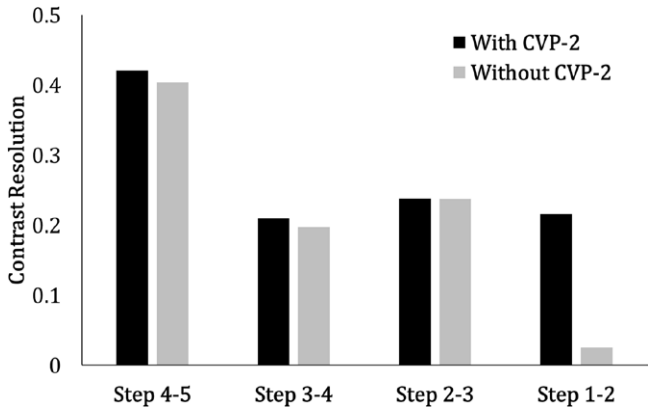

Figure 7. CR of the acryl step function from the C-arm fluoroscope with and without the scattered radiation protector.

concerns regarding the weight and toxicity of lead and its association with environmental and human-health hazards (Christodoulou *et al* 2003, Yue *et al* 2009, Politi *et al* 2012, Kazempour *et al* 2015). These studies showed that lead-free shielding materials possess a good shielding ability, and are environmentally friendly. However, because these alternatives are two to three times more expensive that the traditional lead-shield garment, they have not been widely used. The International Commission on Radiological Protection recommended the use of radiation shielding screens for the protection of workers using fluoroscopy machines in operating rooms without hindering the clinical task (Rehani *et al* 2010). However, the practical use of radiation shielding screens for occupational protection is difficult. Therefore, we think that the newly developed scattered radiation protection device can replace the other protective equipment to decrease the amount of radiation exposure for the surgeon or patient from direct emission or scattered radiation.

Our experiment found that the lowest equivalent scattered radiation doses were delivered to the surgeon's radiosensitive organs if the scattered radiation protector was used for the standard PA configuration. Regarding the direct radiation exposure to the patient, the PA C-arm configuration with CVP-2 also represented an optimal scenario. Until now, there has been no way to decrease the direct radiation exposure to patients, though the development of the scattered radiation protector might solve this problem. For the AP configuration, the scattered radiation protector reduced the scattered radiation doses to the eye (by 44%) and the thyroid (by 57%) more drastically than it reduced the dose to the gonad (by 37%). On the other hand, for the PA configuration, the scattered radiation protector decreased the scattered radiation dose to the gonad (by 37%) more drastically than it reduced the doses to the eye (by 28%) and the thyroid (by 29%). In addition, the scattered radiation doses to the eye and thyroid were lower without the scattered radiation protector for the PA configuration than those with the scattered radiation protector for the AP configuration. The reason for these findings may be

that the eye and thyroid are closer to the x-ray tube for the AP C-arm configuration, whereas the gonad is closer to the x-ray tube for the PA configuration. Therefore, clinicians should be aware that the efficacy of the scattered radiation protector (in terms of mitigating the scattered radiation dose to sensitive organs) can be affected by the configuration of the C-arm fluoroscope, as well as the location of the organs in question.

The scatter map from our results indicates that the scattered radiation protector can reduce the scatter radiation exposure at all locations in the operation room for both PA and AP C-arm configurations. In addition, the scattered radiation dose decreased as the distance from the chest phantom increased, as shown in a previous study (Lee *et al* 2012, Park *et al* 2012). Therefore, other medical staff can also reduce scattered radiation doses by using the scattered radiation protector, or by moving away from the surgical field.

The most important requirement in the development of the scattered radiation protector was that there should be no change in the image clarity of the C-arm fluoroscope. A secondary requirement was that the required exposure conditions should not be noticeably increased upon installing the scattered radiation protector. In the current study, we found no change in the image quality and no increase in the required exposure conditions upon using the scattered radiation protector. Furthermore, the CR improved in step 1 as a result of installing the scattered radiation protector; the scattered radiation protector did not affect the quality of the C-arm fluoroscopic images in the other steps. This result indicates that the ability to distinguish between differences in intensity in thin materials was higher with the scattered radiation protector than without it.

Conclusions

The newly developed scattered radiation protector was effective in reducing not only the equivalent doses from scattered radiation to the surgeon's radiosensitive organs, but also the direct radiation dose to the patient. This was all achieved without decreasing the quality of C-arm fluoroscopic images. Therefore, we recommend the use of this device during intraoperative use of C-arm fluoroscopy.

Acknowledgments

The authors have no conflicts of interest.

This study was supported by the Ministry of Trade, Industry, and Energy of Korea (Grant No. 10045220) and by Korea University Grant (Grant No. K1605461).

References

Athwal G S, Bueno R A Jr and Wolfe S W 2005 Radiation exposure in hand surgery: mini versus standard C-arm *J. Hand Surg. Am.* **30** 1310–6

Bertolini M, Benecchi G, Amici M, Piola A, Piccagli V, Giordano C and Nocetti L 2016 Attenuation assessment of medical protective eyewear: the AVEN experience *J. Radiol. Prot.* **36** 279–89

Biswas D, Bible J E, Bohan M, Simpson A K, Whang P G and Grauer J N 2009 Radiation exposure from musculoskeletal computerized tomographic scans *J. Bone Joint Surg. Am.* **91** 1882–9

Christodoulou E G, Goodsitt M M, Larson S C, Darner K L, Satti J and Chan H P 2003 Evaluation of the transmitted exposure through lead equivalent aprons used in a radiology department, including the contribution from backscatter *Med. Phys.* **30** 1033–8

Das C J, Baliyan V and Sharma S 2015 Image-guided urological interventions: what the urologists must know *Indian J. Urol.* **31** 202–8

Dawe E J, Fawzy E, Kaczynski J, Hassman P and Palmer S H 2011 A comparative study of radiation dose and screening time between mini C-arm and standard fluoroscopy in elective foot and ankle surgery *Foot Ankle Surg.* **17** 33–6

Gavit L, Carlier S, Hayase M, Burkhoff D and Leon M B 2007 The evolving role of coronary angiography and fluoroscopy in cardiac diagnosis and intervention *EuroIntervention* **2** 526–32

Giordano B D, Baumhauer J F, Morgan T L and Rechtine G R 2nd 2009 Patient and surgeon radiation exposure: comparison of standard and mini-C-arm fluoroscopy *J. Bone Joint Surg. Am.* **91** 297–304

Giordano B D, Ryder S, Baumhauer J F and Digiovanni B F 2007 Exposure to direct and scatter radiation with use of mini-C-arm fluoroscopy *J. Bone Joint Surg. Am.* **89** 948–52

Goren A D, Prins R D, Dauer L T, Quinn B, Al-Najjar A, Faber R D, Patchell G, Branets I and Colosi D C 2013 Effect of leaded glasses and thyroid shielding on cone beam CT radiation dose in an adult female phantom *Dentomaxillofac. Radiol.* **42** 20120260

Huang A J 2016 Fluoroscopically guided lumbar facet joint injection using an interlaminar approach and loss of resistance technique *Skeletal Radiol.* **45** 671–6

Kazempour M, Saeedimoghadam M, Shekoohi Shooli F and Shokrpour N 2015 Assessment of the radiation attenuation properties of several lead free composites by Monte Carlo simulation *J. Biomed. Phys. Eng.* **5** 67–76

Lee K, Lee K M, Park M S, Lee B, Kwon D G and Chung C Y 2012 Measurements of surgeons' exposure to ionizing radiation dose during intraoperative use of C-arm fluoroscopy *Spine* **37** 1240–4

Lee M C, Stone N E 3rd, Ritting A W, Silverstein E A, Pierz K A, Johnson D A, Naujoks R, Smith B G and Thomson J D 2011 Mini-C-arm fluoroscopy for emergency-department reduction of pediatric forearm fractures *J. Bone Joint Surg. Am.* **93** 1442–7

Lee S Y, Min E, Bae J, Chung C Y, Lee K M, Kwon S S, Park M S and Lee K 2013 Types and arrangement of thyroid shields to reduce exposure of surgeons to ionizing radiation during intraoperative use of C-arm fluoroscopy *Spine* **38** 2108–12

Lyra M, Charalambatou P, Sotiropoulos M and Diamantopoulos S 2011 Radiation protection of staff in ^{111}In radionuclide therapy—is the lead apron shielding effective? *Radiat. Prot. Dosim.* **147** 272–6

Mesbahi A and Rouhani A 2008 A study on the radiation dose of the orthopaedic surgeon and staff from a mini C-arm fluoroscopy unit *Radiat. Prot. Dosim.* **132** 98–101

Miller D L, Vano E, Bartal G, Balter S, Dixon R, Padovani R, Schueler B, Cardella J F, De Baere T, Cardiovscular, Interventional Radiology Society of Europe and Society Of Interventional Radiology 2010 Occupational radiation protection in interventional radiology: a joint guideline of the Cardiovascular and Interventional Radiology Society of Europe and the Society of Interventional Radiology *Cardiovasc. Intervent. Radiol.* **33** 230–9

Park M S, Lee K M, Lee B, Min E, Kim Y, Jeon S, Huh Y and Lee K 2012 Comparison of operator radiation exposure between C-arm and O-arm fluoroscopy for orthopaedic surgery *Radiat. Prot. Dosim.* **148** 431–8

Politi L, Biondi-Zoccai G, Nocetti L, Costi T, Monopoli D, Rossi R, Sgura F, Modena M G and Sangiorgi G M 2012 Reduction of scatter radiation during transradial percutaneous coronary angiography: a randomized trial using a lead-free radiation shield *Catheter. Cardiovasc. Interv.* **79** 97–102

Prince J L and Links J M 2006 *Medical Imaging Signals and Systems* (Upper Saddle River, NJ: Pearson Prentice Hall)

Rehani M M, Ciraj-Bjelac O, Vano E, Miller D L, Walsh S, Giordano B D and Persliden J 2010 ICRP Publication 117. Radiological protection in fluoroscopically guided procedures performed outside the imaging department *Ann. ICRP* **40** 1–102

Rubesin S E, Levine M S, Laufer I and Herlinger H 2000 Double-contrast barium enema examination technique *Radiology* **215** 642–50

Shoaib A, Rethnam U, Bansal R D A and Makwana N 2008 A comparison of radiation exposure with the conventional versus mini C arm in orthopedic extremity surgery *Foot Ankle Int.* **29** 58–61

Shortt C P, Fanning N F, Malone L, Thornton J, Brennan P and Lee M J 2007 Thyroid dose during neurointerventional procedures: does lead shielding reduce the dose? *Cardiovasc. Intervent. Radiol.* **30** 922–7

Sung K H, Min E, Chung C Y, Jo B C, Park M S and Lee K 2016 Measurements of surgeons' exposure to ionizing radiation dose: comparison of conventional and mini C-arm fluoroscopy *J. Hand Surg. Eur.* **41** 340–5

Tuohy C J, Weikert D R, Watson J T and Lee D H 2011 Hand and body radiation exposure with the use of mini C-arm fluoroscopy *J. Hand Surg. Am.* **36** 632–8

US Food and Drug Administration 2016 *Establishment Registration & Device Listing* (online) Available: www.accessdata.fda.gov/scripts/cdrh/cfdocs/cfRL/rl.cfm (Accessed: 31 July 2016)

Yue K, Luo W, Dong X, Wang C, Wu G, Jiang M and Zha Y 2009 A new lead-free radiation shielding material for radiotherapy *Radiat. Prot. Dosim.* **133** 256–60